Eur. Phys. J. D **31**, 451–457 (2004)
DOI: 10.1140/epjd/e2004-00168-1

THE EUROPEAN PHYSICAL JOURNAL D

Temperature measurement of a single ion in a Penning trap

S. Djekic[1], J. Alonso[1,2], H.-J. Kluge[2], W. Quint[2], S. Stahl[1], T. Valenzuela[1], J. Verdú[1], M. Vogel[1,a], and G. Werth[1]

[1] Institut für Physik, Johannes-Gutenberg-Universität, 55099 Mainz, Germany
[2] GSI, 64291 Darmstadt, Germany

Received 9 March 2004 / Received in final form 8 July 2004
Published online 6 December 2004 –

Abstract. The present work is concerned with the association of a temperature to a single ion stored in a Penning ion trap. Several methods are described which allow to determine the temperature by measurements of the ion's cyclotron and axial trapping frequencies. Recent results of a measurement on a hydrogen-like carbon ion $^{12}C^{5+}$ by use of mode coupling are presented and possible further applications are discussed.

PACS. 07.20.-n. Thermal instruments and apparatus – 07.20.Dt. Thermometers – 42.50.Lc Quantum fluctuations – 42.50.Vk Mechanical effects of light on ions

1 Introduction

The concept of temperature is usually applied only to large ensembles of particles. However, under certain conditions the concept of temperature can be given a meaning also with individual particles. It has, for example, been successfully applied to a single electron confined in a Penning trap [1]. Generally, in the case of a thermal equilibrium with the environment at a temperature T, if one measures the motional energy E of an individual particle repeatedly, the probability of obtaining a certain value for the energy follows the exponential $\exp(-E/k_BT)$, where k_B is the Boltzmann constant. It therefore represents a Boltzmann distribution which is characterized by a temperature. However, this is valid only under the assumption that the system is ergodic [2]. This assumption states that the result of a measurement of an observable performed over an ensemble of particles, if averaged, yields the same result as given by several consecutive measurements of the same observable on a single particle, time-averaged.

If the system is indeed ergodic and there is a thermal equilibrium between the environment and the particle, this yields the possibility of utilizing an ion's trapping motion as a probe for thermometry. A single charged particle in a Penning trap [3] interacts via electromagnetic forces with the electrodes of the trap which are coupled to attached electronic circuits used for detection of the ion's trapping motions. It is well-known [4] that the ion's movement in the trap induces image currents in the trap electrodes and thus in the attached electronics, as represented schematically in Figure 1. Since the nature of the coupling forces is bidirectional, thermal fluctuations in the electronics due to thermal charge carrier motion also affect the ion's movement in the trap. The strength of this coupling can be expressed in terms of a time constant τ with which the exponential energy loss of an excited ion would take place. It is given by [5]

$$\tau = \frac{m}{q^2}\frac{D^2}{R}, \tag{1}$$

where m is the ion mass and q is its electric charge. D is the so-called effective distance between the signal pickup electrodes and R is the corresponding resistance. Equilibrium between the temperature of the electronics and the ion's motion is reached after a time $t \gg \tau$.

The amplitude of a trapping motion is a direct measure for the corresponding energy. In an ideal Penning trap [4], the amplitudes of the three trapping motions are not coupled and therefore every degree of freedom of the ion can independently be attributed with a different temperature. Trap imperfections as, e.g., geometrical deviations from the ideal case will lift this degeneracy to a certain degree,

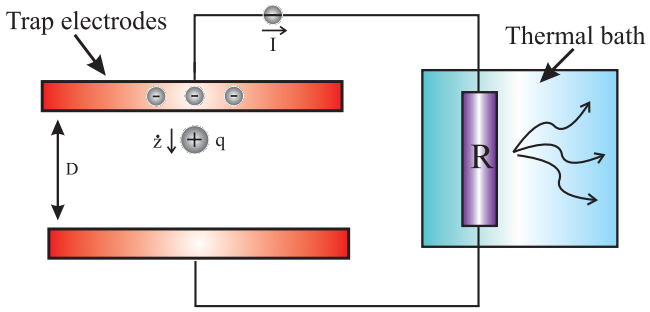

Fig. 1. Schematic view on the interaction of the ion motion with the trap electrodes and resonance circuits.

[a] e-mail: manuel.vogel@uni-mainz.de

however not necessarily strong enough to compensate for the different energy dissipations into the system, e.g., due to different external noise levels in the respective resonance circuits. Therefore, even in an imperfect trap, different thermal equilibria can develop in different motional degrees of freedom of the ion. In the present case, the axial and cyclotron degrees of freedom have distinct motional frequencies in resonance with precisely tuned circuits of high quality factors. Note, that it is the charge carrier temperature of the electrodes and the electronics that is predominantly relevant for the present investigations. The association of a temperature to the magnetron degree of freedom is possible only when the particle can be in a thermal equilibrium with its surrounding and still be stored. This will commonly not be the case, since the radius of the magnetron motion increases with decreasing energy and in a liquid helium surrounding as in the present case, the corresponding radius is much larger than the trap, thus leading to particle loss.

Accurate knowledge of a single particle's motional temperature in the Penning trap is relevant for high-precision measurements of any quantity that depends on the particle's dynamics. As pointed out in [6], knowledge of the single ion's temperature is of importance e.g. for the lineshape of the spin-flip resonance used for the determination of the particle's g-factor and influences the precision of such measurements directly.

In the following, we will restrict the discussion to the determination of the temperature associated with the cyclotron and the axial trapping motion. Several possible approaches to the determination of the axial temperature will be discussed.

2 A single ion in a Penning trap

A single hydrogen-like ion $^{12}C^{5+}$ is used in the present experiments. The choice of this ion is arbitrary and not of special interest for the present investigations. The ion is prepared by electron impact ionization of the neutral species and subsequent trapping of the ionization products. Mass and charge state selection is then performed by ejection of all unwanted species from the trap. Repeated lowering of the trapping potential leads to stepwise ion loss until only a single ion remains trapped. The ion signal is picked up by resonant circuits attached to the trap electrodes which are tuned to the respective motional frequencies of the ion under investigation. Thus, motional frequencies and amplitudes can be measured independently.

The three physically realized motional frequencies in the trap are the so-called "perturbed cyclotron frequency", the axial frequency and the "magnetron frequency". The perturbed cyclotron frequency is given by

$$\omega_+ = \frac{\omega_c}{2} + \sqrt{\frac{\omega_c^2}{4} - \frac{\omega_z^2}{2}} \tag{2}$$

where ω_c is the free cyclotron frequency of the ion in the magnetic field of the trap, $\omega_c = (q/m)B$. B is the magnetic field strength and ω_z is the "axial frequency" of the oscillation along the magnetic field lines given by

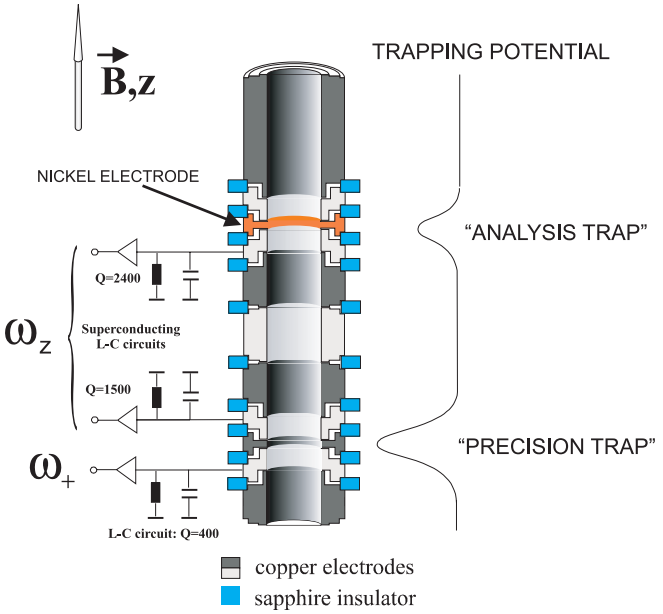

Fig. 2. Schematic representation of the double trap set-up used for the present investigations.

$$\omega_z = \sqrt{\frac{qU}{md^2}}, \tag{3}$$

where d is the characteristic trap parameter [7]. The "magnetron frequency" is given by

$$\omega_- = \frac{\omega_c}{2} - \sqrt{\frac{\omega_c^2}{4} - \frac{\omega_z^2}{2}} \tag{4}$$

and is an unstable drift motion around the trap center in the combined electric and magnetic field of the trap. The axial motion is due to the electric potential minimum between the trap endcaps and thus independent of B. Typical values for ω_+, ω_- and ω_z in the present experiment are 25 MHz, 16 kHz and 1 MHz, respectively, with an accuracy of the axial frequency measurement of about 50 mHz.

The details of the experimental set-up and procedures are given in [8,9]. Figure 2 is a schematic representation of the double trap set-up used for the present investigations. The trap electrodes are shown together with the electronic resonance circuits used for the detection of the respective ion motions. Details will be discussed below. This double-trap arrangement is also successfully used for highly precise measurements [6,8,9,12–14] of the magnetic moment of single highly charged ions by use of the continuous Stern-Gerlach effect [8,9]. The traps differ mainly in the existence of an artificial magnetic field inhomogeneity due to the presence of a nickel ring in the so-called "analysis trap" (see Fig. 2). This inhomogeneity causes a frequency shift between the different spin states of the electron bound in the hydrogen-like ion and thus allows for a determination of its magnetic moment by means of the continuous Stern-Gerlach effect. The remaining magnetic field inhomogeneity in the second trap, the so-called

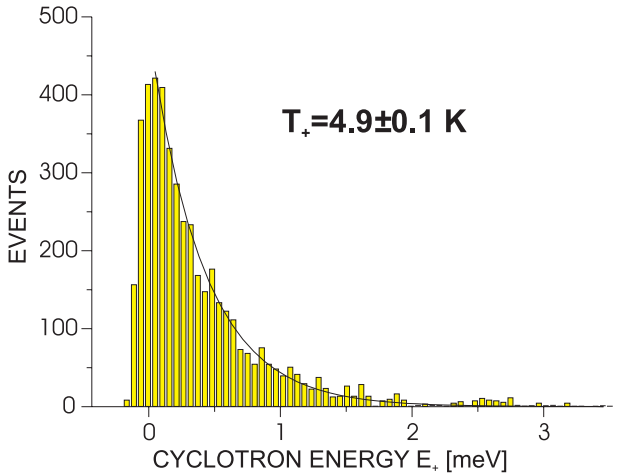

Fig. 3. Measured distribution of the cyclotron energy E_+ yielding a cyclotron temperature of 4.9 ± 0.1 K (from [8]).

"precision trap" is three orders of magnitude smaller and thus allows for a precise measurement of the ion's motions.

3 Cyclotron temperature measurement

The cyclotron temperature can be measured by coupling of the axial and cyclotron motions in an inhomogeneous magnetic field. As stated above, the nickel ring electrode of our analysis trap produces a bottle-like magnetic field which can be characterized by a series expansion

$$B(z) = B_0 + B_1 z + B_2 z^2 + \ldots \tag{5}$$

Odd terms vanish because of the mirror symmetry of the field. The coupling of axial and cyclotron motions leads to an axial frequency shift $\Delta\omega_z$ for a given cyclotron energy E_+ [4]:

$$E_+ = m\omega_z \frac{B_0}{B_2} \Delta\omega_z. \tag{6}$$

In our case $B_0 = 3.8$ T and $B_2 = 8.2(9)$ mT/mm^2. The corresponding shift in ω_z has been determined experimentally by systematic excitation of the cyclotron energy to 5 Hz per meV [8,9].

Figure 3 shows the distribution of the thermally fluctuating cyclotron energy E_+ as obtained from a repeated measurement of the axial frequency ω_z in the analysis trap. The axial frequency is measurement by signal pickup of the oscillating ion's mirror charges with a tuned resonance circuit attached to the corresponding trap electrodes (see Fig. 2) and subsequent Fourier analysis of the signal. A least squares fit to a Boltzmann distribution yields a cyclotron temperature $T_+ = 4.9 \pm 0.1$ K. This temperature is slightly higher than the ambiance temperature of 4.2 K from the liquid He bath due to additional noise originating from the trap voltage supplies. The small tail of the measured distribution for $E_+ < 0$ also results from this noise and the corresponding axial frequency uncertainty.

4 Axial temperature measurement

The axial temperature measurement is based on repeated measurement of the axial energy for a given ambiance temperature and the calculation of the mean value of the resulting distribution. This is not as straight-forward as in the cyclotron case discussed before, since the axial frequency to first order does not depend on the value of the axial energy. We present three different approaches to the determination of the axial temperature and apply them to a single stored hydrogenic carbon ion $^{12}C^{5+}$.

4.1 Active methods

4.1.1 Active sideband coupling

This method for measuring the axial temperature has been described earlier by Häffner et al. [9]. It is based on a coupling of the cyclotron motion to the axial motion by an rf field at the frequency $\omega_+ - \omega_z$ applied in the radial plane of the trap between different segments of the split ring electrode in the precision trap. The effect of this coupling is to make the quantum numbers of both oscillations identical. For a detailed description of this effect, see [10,11]. Then we have the relation

$$\frac{E_+}{\omega_+} = \frac{E_z}{\omega_z} \tag{7}$$

between the cyclotron and axial energies. This can be used to determine the axial energy from a measurement of the cyclotron energy. When the cooling time constant of the axial motion is much smaller than the cyclotron cooling time constant, then the axial energy fixes the cyclotron energy. The axial motion first reaches equilibrium with the environment by resistive cooling. To ensure the equivalence of the quantum numbers the sideband coupling is performed during a time of around 10 s, which is about 100 times longer than the corresponding energy exchange time. The cyclotron energy is measured as described in Section 3 by monitoring the axial frequency in an inhomogeneous magnetic field for a sufficiently long time of e.g. several hours, performing measurements every few seconds. To that end, the ion has to be transported to a magnetic bottle ("analysis trap" in Fig. 2) which shifts the axial frequency when the cyclotron energy changes due to thermal fluctuations as described in Section 3. When E_+ is known we obtain the axial temperature by

$$T_z = \frac{\langle E_z \rangle}{k_B} = \frac{\langle E_+ \rangle}{k_B} \frac{\omega_z}{\omega_+}. \tag{8}$$

In our measurement (see Fig. 4) we found an axial temperature of $T_z = 61 \pm 9$ K. A more detailed discussion of this method can be found in [15].

The main disadvantage of this method is the fact that the ion has to be transported from a homogeneous B field region to a magnetic bottle with a known (measured) B_2 term, which requires the assumption that the transport is an adiabatic process, i.e. there is no temperature

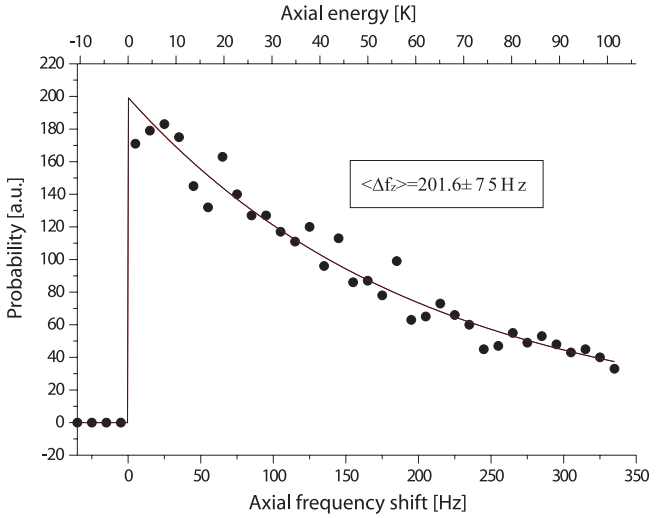

Fig. 4. Cyclotron energy Boltzmann distribution result of the measurement by active sideband cooling, yielding an axial temperature of $T_z = 61 \pm 9$ K.

(energy) variation during the transport. Energy loss due to radiative cooling by synchrotron radiation can be excluded in the present case. Under the given conditions the maximum cooling rate of a trapped ion is given by the radiated power

$$P = \frac{1}{6\pi\epsilon_0}\frac{q^6}{c^3}\frac{B^4}{m^4}r^2, \tag{9}$$

where c is the speed of light and r is the ion's motional amplitude. For typical parameters in the present experiment, the radiated power P is on the order of 10^{-6} eV/s. Therefore, radiative energy loss during typical transport times of 100 milliseconds can be neglected. However, the transport process might be not completely adiabatic due to other energy dissipation processes e.g. due to electric potential switching during transport or due to magnetic field changes.

4.1.2 Active motional excitation

In this case, the measurement procedure is similar to the method explained in Section 4.1.1 in the sense that the axial temperature is also obtained by means of actively coupling the axial and the cyclotron motions, only that now there is no need of transporting the ion to the magnetic bottle. Still, the remaining magnetic field inhomogeneity as expressed by B_2 can be used for a measurement of the axial temperature, even though in the present case it is smaller by three orders of magnitude. The associated constraint is that one can no longer count only on the direct relationship between the cyclotron energy and the axial frequency shift (Eq. (6)) to determine the axial energy. This is because the axial frequency shift depends on the value of the B_2 term, which in the magnetic bottle is big enough to make thermal variations of the cyclotron energy visible as axial shifts, but not so in the by three orders of magnitude more homogeneous B field. Thus, by external excitation the axial temperature has to be increased by a well-known factor for the axial frequency shift to be big enough to be resolved. This is achieved as follows: First, the ion motion is resistively cooled until it reaches a thermal equilibrium with the surroundings. This is the temperature associated with the minimum attainable axial energy for the current set-up, denoted by T_0, and also the temperature that is aimed to be determined. Then an axial frequency measurement is carried out ($\omega_{z_{cold}}$) and a measurement of the background Johnson noise level (U_{n_0}) in a frequency window around this axial frequency is performed. The axial motion is excited to increase the corresponding temperature to a higher value T_1 . Once this rise has occurred, the axial and cyclotron motions are coupled by use of the method described in Section 4.1.1 and a net energy transfer from the axial to the cyclotron degree of freedom takes place. Then the background Johnson level is measured with the applied excitation, yielding a value for U_{n_1} typically 5 times bigger than U_{n_0}. Finally, a second axial frequency measurement is performed, yielding $\omega_{z_{hot}}$.

If one now substitutes the known parameters in equation (6) by its numerical values ($m = 12\,u$, $\omega_z = 2\pi \times 916.97$ kHz, $B_0 = 3.797$ T and $B_2 = 8.2\ \mu\mathrm{T/mm^2}$), it results in

$$E_+ \approx 2\pi \times 2.085 \Delta\omega_z. \tag{10}$$

A value for the cyclotron energy is obtained with the measured quantity for the frequency shift

$$\Delta\omega_z = \omega_{z_{hot}} - \omega_{z_{cold}}. \tag{11}$$

By repeating this procedure many times one obtains the Boltzmann distribution of the cyclotron energy.

As in the first method, explained in Section 4.1.1, by making use of the fact that the quantum numbers of both the axial and cyclotron motion are made equal by sideband coupling, a direct relationship between the mean values of both energy distributions can be found:

$$\frac{\langle E_z\rangle}{\omega_z} = \frac{\langle E_+\rangle}{\omega_+}. \tag{12}$$

Since the mean value of the Boltzmann distribution is given by $k_B T$ and since it can be directly derived from an exponential fit to the experimental results, equation (12) becomes

$$T_1 = \frac{\omega_z}{\omega_+}\frac{\langle E_+\rangle}{k_B} \tag{13}$$

from where one determines the axial temperature of the ion during the excitation.

The final step is to obtain a proportionality factor between T_1 and T_0. For this purpose, the Johnson noise levels at both temperatures have been measured. The expression that relates the Johnson noise level (U_n) to the temperature (T) of a system is [16]

$$U_n^2 = 4k_B T B_f R \tag{14}$$

where B_f is the frequency bandwidth under observation. Therefore, the initial axial temperature can be found as

$$T_0 = \frac{\omega_z}{\omega_+}\frac{\langle E_+\rangle}{k_B}\frac{U_{n0}^2}{U_{n_1}^2}. \tag{15}$$

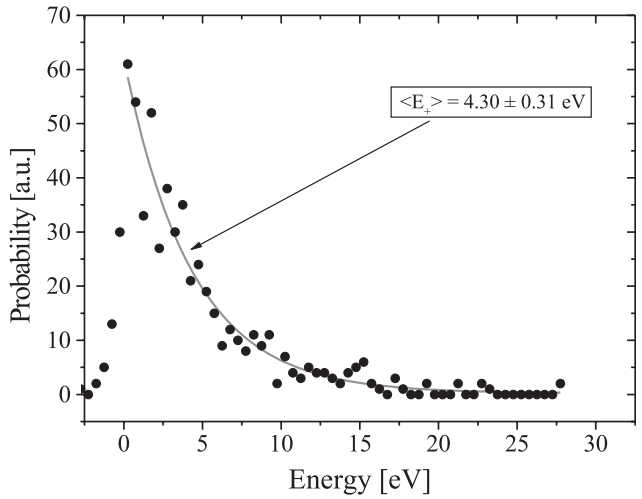

Fig. 5. Plot of the Boltzmann distribution of the cyclotron energy.

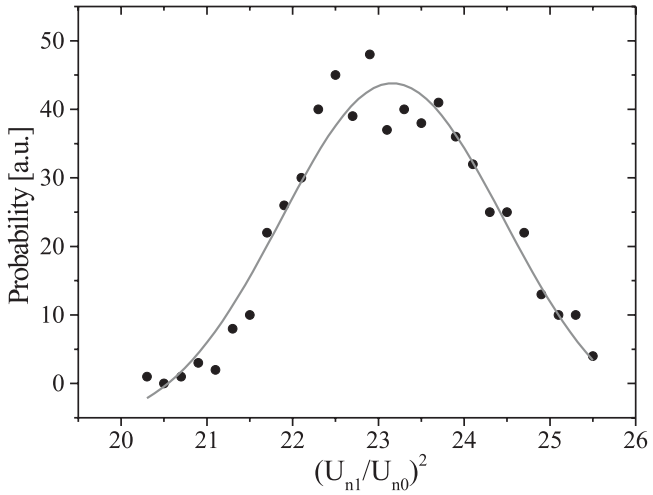

Fig. 6. Distribution of the proportionality constant which defines the ratio T_1/T_0. The solid line is a Gaussian fit to the data, yielding a mean value of $U_{n_1}^2/U_{n_0}^2 = 23.2 \pm 1.3$.

The resulting curve for the distribution of the cyclotron energy upon axial excitation and mode coupling is plotted in Figure 5, yielding a mean value of

$$\langle E_+ \rangle = 4.03 \pm 0.31 \text{ eV} \tag{16}$$

where the uncertainty is purely statistically determined by the least square fit.

The next number needed for the calculation of T_0, is $U_{n_1}^2/U_{n_0}^2$. Statistical fluctuations of this repeatedly measured quantity shows a Gaussian distribution, as can be seen in Figure 6. It introduces the largest uncertainty in the final number for the axial temperature measurement. It amounts to a value of

$$\left\langle \left(\frac{U_{n_1}}{U_{n_0}} \right)^2 \right\rangle = 23.2 \pm 1.3 \tag{17}$$

with these numbers and the axial and cyclotron frequencies ($\omega_z = 2\pi \times 916.97$ kHz and $\omega_+ = 2\pi \times 24.076$ MHz, with associated uncertainties too small in comparison to $\langle E_+ \rangle$ and $U_{n_1}^2/U_{n_0}^2$ to be considered), one gets a value from equation (15) for the axial temperature of the single hydrogenic carbon ion of

$$T_0 = 77 \pm 6 \pm 8 \text{ K}, \tag{18}$$

where the first uncertainty comes from statistical considerations and the second one from the uncertainty in the value measured for B_2 [15]. One can see that in Figure 5 there are some points hinting at negative energies corresponding to negative axial frequency shifts. These negative shifts arise from the fact that for the determination of the cyclotron energy we are assuming that the substraction of two Boltzmann distributions (corresponding to $\omega_{z_{hot}}$ and $\omega_{z_{cold}}$) gives another Boltzmann distribution. This is, of course, not true. However, the ratio in the two mean values for the axial distributions is so high, that the difference actually resembles a characteristic exponential, save for the small tail appearing for negative energy values.

4.2 Passive method: residual motional coupling

A second possibility for an axial temperature measurement is making use of the fact that the trapping potential can be chosen not to be completely harmonic. The axial frequency will in this case depend on the axial energy and the lineshape of the ion's resonance signal will be nonsymmetric.

Then the electric potential Φ along the symmetry axis of the trap (i.e. the z-direction) has a nonvanishing octupole term C_4 in the expansion of the potential

$$\Phi(z,0) = \sum_{j=0}^{\infty} C_j z^j \; ; \quad C_j = \frac{1}{j\,!} \frac{\partial^j \Phi}{\partial z^j}\Big|_{(0,\,0)}. \tag{19}$$

In the present set-up, the harmonicity of the trapping potential can be influenced by the choice of the voltages applied to correction electrodes of the Penning trap placed symmetrically between the ring and endcap electrodes. This is expressed in terms of the so-called "tuning ratio" tr, which is the ratio of the voltages applied to the correction electrodes and the ring electrode. The term C_4 appears due to the deviation from an ideal, infinite hyperbolical trap. It is related to the difference between the optimal tuning ratio (i.e. the one to achieve a harmonic trap potential) and the one actually applied. For the present trap set-up, this relation is calculated to be [17]

$$C_4 = \frac{1}{4!} \sum_{m=1,3,5}^{\infty} \left(\frac{m\pi}{L} \right)^4 (A_m + B_m \; tr), \tag{20}$$

where L is the length of the cylindrical trap and A_m and B_m are tuning ratio parameters which are calculated by use of the given trap geometry [17]. The dependence of the axial frequency on the axial energy can be written as

$$\omega_z = \omega_{z,E_z=0} + \beta E_z \tag{21}$$

where $\omega_{z,E_z=0}$ is the axial frequency for vanishing axial energy. β is given by

$$\beta = \frac{C_4}{(C_2)^2} \frac{3\omega_z}{8\pi\, q\, U} \tag{22}$$

and describes the dependence of the axial frequency ω_z on the axial energy E_z in terms of the determined C_4.

By fixing a non-optimized tuning ratio and measuring the axial resonance signal of the ion, the motional temperature can be extracted from the lineshape of the resonance signal. To that end, the lineshape for a fixed axial energy E_z of the ion is convoluted with a Boltzmann distribution of that energy to describe the smearing out of the resonance due to thermal energy fluctuations. Thus, one starts with a Lorentz-type lineshape as given by

$$U(\omega_z) \propto \sqrt{\frac{(\omega_{z,r} - \omega_z)^2}{\gamma^2/4 + (\omega_{z,r} - \omega_z)^2}} \tag{23}$$

where $U(\omega_z)$ is the measured FFT signal voltage and $\omega_{z,r}$ is the resonance frequency of the circuit. γ is the frequency-dependent damping factor due to the impedance $Z(\omega)$ of the system defined by

$$\gamma = \frac{q^2}{mD^2} Z(\omega) = \frac{1}{\tau} \tag{24}$$

in analogy and with the same nomenclature as in equation (1). The convolution of equation (23) with a Boltzmann distribution yields

$$U(\omega_z) \propto \int_0^\infty \exp\left(\frac{-E_z}{k_B T}\right) \times \sqrt{\frac{(\omega_{z,r} - (\omega_z + \beta E_z))^2}{\gamma^2/4 + (\omega_{z,r} - (\omega_z + \beta E_z))^2}} dE_z. \tag{25}$$

Thus, by numerical inversion of equation (25) a value for the axial energy (and therefore temperature) can be found for a given (measured) axial resonance curve at a fixed detuning of the trap.

Figure 7 shows a measured resonance curve together with the fitted curve according to equation (25) yielding an axial temperature of 62 ± 10 K. Similar measurements have been performed for a number of values for the detuning. The combined result for the axial temperature is 69 ± 8 K.

This method does not require transport of the ion, but has the disadvantage that the numbers in equations (20) and (21) have been calculated for ideal trap geometry and may vary due to any geometrical imperfections or charge accumulation on the electrodes. However, an accurate measurement by other methods will yield an experimental value for C_4 through equations (20) and (21).

5 Direct noise temperature measurement

Assuming the equality of the noise temperature of the resonance circuit attached to the trap and the ion inside the trap, a value for the ion's temperature can be obtained by a measurement of the noise temperature of the electronics. To that end, the Johnson noise level voltage U_n of the electronics has been measured by use of a Yokogawa SA2400 spectrum analyzer upon frequency downconversion of the signal. An absolute value of the noise level has been calculated by use of the corresponding attenuation factor between the resonance circuit and the spectrum analyzer. This number (i.e. the transfer function) has been determined by a combination of measured attenuation factors and calculations based on the known electronic properties of the relevant components.

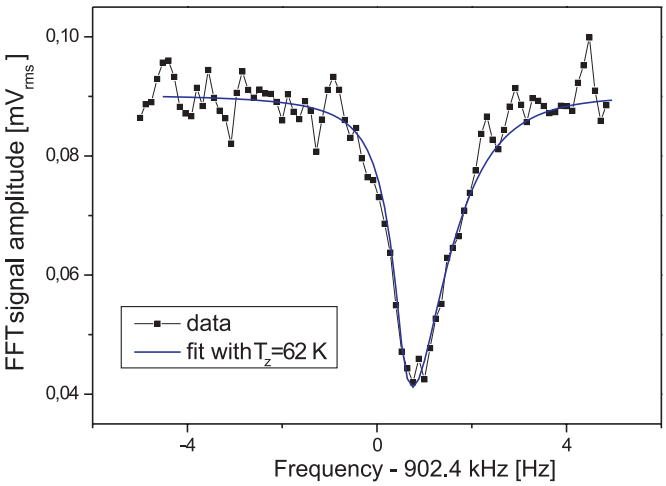

Fig. 7. Measured axial resonance signal (data points) and fitted curve according to equation (25) yielding an axial temperature $T_z = 62$ K.

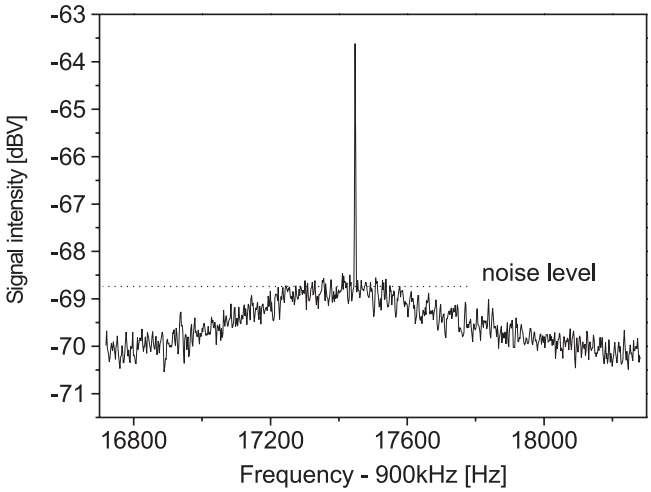

Fig. 8. Noise spectrum of the axial detection circuit. The sharp peak marks the frequency at which the noise level voltage is to be determined.

Figure 8 shows a measured noise spectrum of the axial detection circuit. The sharp peak marks the frequency at which the noise level voltage is to be determined. The expression that relates this Johnson noise level (U_n) to the temperature (T) of a system is given by equation (14)

and can be solved to give

$$T = \frac{U_n^2}{4k_B B_f R} \tag{26}$$

with the same nomenclature as above. The observation bandwidth has been chosen to be $B_f = 7.8\,\mathrm{Hz}$. The resistance R of the resonance circuit is determined from the measured quality factor Q by

$$R = \frac{Q}{\omega_r C} \tag{27}$$

where C is the capacitance of the resonance circuit. Corrections to this value have to be made due to the existence of attached electronics which have been taken into account by a corresponding simulation. It yields a resistance R of 11.0 ± 1.4 MΩ at a capacity of $C = 23 \pm 3$ pF. With this, the resulting value for the noise temperature is $T = 52 \pm 5 \pm 3\,\mathrm{K}$, where the first uncertainty is the statistical measurement uncertainty and the second one is due to the uncertainties in R and C used in the simulation.

6 Conclusion

We have presented different approaches to measure the temperature of a single ion confined in a Penning trap and have applied these methods to the cyclotron and the axial motion of the ion. While the measured cyclotron temperature of $T_+ = 4.9 \pm 0.1\,\mathrm{K}$ is in satisfactory agreement with the liquid helium surrounding, the resulting value for the axial temperature is significantly higher. Measurements performed on a single, hydrogen-like carbon ion $^{12}C^{5+}$ have yielded results which agree within the given uncertainties and give a combined value of $T_z = 69 \pm 6\,\mathrm{K}$. Since the different approaches are based on different aspects of the trapping, a combination of the presented methods can be used for an experimental determination of certain trapping parameters, as e.g. trapping potential anharmonicity terms and electronic noise levels.

A direct measurement of the electronic noise temperature of the electronics attached to the trap electrodes has yielded a value of $T_z = 52 \pm 5 \pm 3\,\mathrm{K}$, in fair agreement with the value determined from the ion's motion.

Such a deviation of the axial ion temperature from the liquid helium ambiance temperature of about 4 K has been commented on before [18]. It is most likely due to noise in the electronic components used for axial signal detection. These are different from the electronics used for cyclotron signal detection mainly with respect to the quality factor and frequency of the resonance circuit and the subsequent mixing and amplification of the signal.

The highest measured ion temperature is the one determined by active sideband excitation (see Sect. 4.1.2). This higher temperature as compared to the electronic noise temperature in the axial degree of freedom might be due to parasitic sideband excitation. The irradiated sideband frequency $\omega_+ - \omega_z$ used for coupling the ion motions is close to the cyclotron frequency itself and might thus excite the cyclotron degree of freedom and therefore also the axial degree of freedom above its original value.

Apparently, the residual coupling of the axial motion due to e.g. trap imperfections to the other degrees of freedom is not strong enough to produce a thermal equilibrium amongst all degrees of freedom at the axial temperature. This is already clear from the fact that the cyclotron temperature T_+ has been measured to be 4.9 K in agreement with the ambiance temperature while the axial temperature T_z is more than one order of magnitude higher.

From the fact that the measured energy distributions obey a Boltzmann distribution it may be concluded that the system under investigation (i.e. the single ion in interaction with the trap electrodes and attached resonance circuits) is an ergodic system in the sense defined before. The ergodicity is connected with the requirement that the particle is able to access the whole available phase space within the measurement time, which apparently is the case here. This seems to be reasonable also if one realizes that the typical motional frequencies are more than six orders of magnitude higher than the inverse measurement time and the ion's motion is in principle unrestricted within the trapping volume, especially since the ion's spatial trajectory is not closed [4].

This work was funded by the BMBF and the EU in the framework of the HITRAP project (grant no. HPRI-CT-2001-50036).

References

1. B. D'Urso, B. Odom, G. Gabrielse, Phys. Rev. Lett. **90**, 043001 (2003)
2. D.A. McQuarrie, *Statistical Mechanics* (Harper and Row, New York, 1976)
3. F.M. Penning, Physica **3**, 873 (1936)
4. L.S. Brown, G. Gabrielse, Rev. Mod. Phys. **58**, 233 (1986)
5. D.J. Wineland, H.G. Dehmelt, J. Appl. Phys. **46**, 919 (1975)
6. J. Verdú et al., Phys. Rev. Lett. **92**, 093002 (2004)
7. G. Gabrielse, L. Haarsma, S.L. Rolston, Int. J. Mass Spectrom. Ion Proc. **88**, 319 (1989)
8. G. Werth, H. Häffner, W. Quint, Adv. At. Mol. Opt. Phys. **48**, 191 (2002)
9. H. Häffner et al., Eur. Phys. J. D **22**, 163 (2003)
10. E.A. Cornell, R.M. Weisskoff, K.R. Boyce, D.E. Prichard, Phys. Rev. A **41**, 312 (1990)
11. M. Kretschmar, AIP Conf. Proc. **457**, 242 (1999)
12. N. Hermanspahn et al., Phys. Rev. Lett. **84**, 427 (2000)
13. H. Häffner et al., Phys. Rev. Lett. **85**, 5308 (2000)
14. J. Verdú et al., J. Phys. B **36**, 655 (2003)
15. H. Häffner, *Präzisionsmessung des magnetischen Moments des Elektrons in wasserstoffähnlichem Kohlenstoff*, Ph.D. thesis, Johannes-Gutenberg-Universität Mainz (2000)
16. J.B. Johnson, Phys. Rev. **32**, 97 (1928)
17. J. Verdú et al., publication in preparation
18. F. DiFilippo et al., Phys. Scripta T **59**, 144 (1995)